HHS Public Access

Author manuscript

J Immunol. Author manuscript; available in PMC 2021 July 15.

Published in final edited form as:

J Immunol. 2020 July 15; 205(2): 377–386. doi:10.4049/jimmunol.1901463.

Loss of the IL-27R Results in Enhanced Tubulointerstitial Fibrosis Associated with Elevated Th17 Responses

Gaia M Coppock[1,2], **Lillian R Aronson**[1,3], **Jihwan Park**[2], **Chengxiang Qiu**[2], **Jeongho Park**[1], **Jonathan H. DeLong**[1], **Enrico Radaelli**[1], **Katalin Suszták**[2], **Christopher A Hunter**[1]

[1]Department of Pathobiology, School of Veterinary Medicine, University of Pennsylvania, Philadelphia, Pennsylvania, United States of America

[2]Renal, Electrolyte, and Hypertension Division, University of Pennsylvania, Philadelphia, Pennsylvania, United States of America

[3]Section of Surgery, Department of Clinical Studies, School of Veterinary Medicine, University of Pennsylvania, Philadelphia, Pennsylvania, United States of America

Abstract

Clinical and experimental studies have established that immune cells such as alternatively activated (M2) macrophages and Th17 cells play a role in the progression of chronic kidney disease (CKD), but the endogenous pathways that limit these processes are not well understood. The cytokine IL-27 has been shown to limit immune-mediated pathology in other systems by effects on these cell types, but this has not been thoroughly investigated in the kidney. Unilateral ureteral obstruction (UUO) was performed on WT and IL-27Rα$^{-/-}$ mice. After two weeks, kidneys were extracted, and the degree of injury was measured by hydroxyproline assay and quantification of NGAL mRNA. Immune cell infiltrate was evaluated by immunohistochemistry and flow cytometry. An anti-IL-17A monoclonal antibody was subsequently administered to IL-27Rα$^{-/-}$ mice every two days from day of surgery with evaluation as described after two weeks. After UUO, IL-27 deficiency resulted in increased tissue injury and collagen deposition, associated with higher levels of chemokine mRNA and increased numbers of M2 macrophages. Loss of the IL-27Rα led to increased infiltration of activated CD4^{+} T cells that co-produced IL-17A and TNFα, and blockade of IL-17A partially ameliorated kidney injury. Patients with CKD had elevated serum levels of IL-27 and IL-17A, while expression of transcripts for the IL-27RA and the IL-17RA mRNA in the tubular epithelial cells of patients with renal fibrosis correlated with disease severity. These data suggest that endogenous IL-27 acts at several points in the inflammatory cascade to limit the magnitude of immune-mediated damage to the kidney.

Keywords

IL-27; kidney fibrosis; inflammation

INTRODUCTION

Chronic kidney disease (CKD), characterized by renal damage and reduced kidney function, affects approximately 14 percent of the general American population and is associated with increased morbidity and mortality as well as high healthcare costs (1). Preventative therapies

are limited, and novel strategies to identify and ameliorate profibrotic processes have important diagnostic and therapeutic implications. The immune system has established relevance in fibrotic disease progression in multiple organs such as lungs, liver, and kidneys (2, 3). In the kidney, damage to the renal tubular epithelial cells leads to the release of damage-associated molecular patterns (DAMPs) that promote innate activation and recruitment of immune cells (2) (3). This process amplifies the inflammatory response in the injured organ, and these events can progress to chronicity and result in immune-mediated fibrosis (3). In multiple models of kidney injury, the increased infiltration of macrophages is associated with renal damage (4–6) and in chronically inflamed kidneys these cells can express the mannose receptor, CD206, and have an alternatively activated (M2) phenotype (4, 7, 8). $CD4^+$ T cells also contribute to the proinflammatory fibrotic processes in the kidney (9, 10), and the ability of Th2 cells to produce IL-4 and IL-13 (which can enhance M2 polarization) is a major factor that promotes fibrosis (11). More recent studies in mouse models have shown that $CD4^+$ T cells that produce interleukin-17 (Th17 cells) contribute to kidney fibrosis and that in patients Th17 cells are associated with fibrotic kidney tissue (12–14). However, many questions remain about the function of IL-17 in the kidney and its contribution to fibrosis.

It has been proposed that the ability to harness natural negative regulators is one method to target immune-mediated fibrotic processes and limit disease progression (15, 16). The cytokine interleukin-27 (IL-27), which is comprised of the subunits IL-27p28 and EBi3, signals through a receptor composed of gp130 and the IL-27Rα and has been shown in various infectious and inflammatory models to limit the magnitude of the immune response (17–20). IL-27 can limit $CD4^+$ Th1, Th2, and Th17 responses and thereby can attenuate immune-mediated pathology in murine models of autoimmune disease and infection (17, 21, 22). Moreover, M2 macrophages have been reported to express the IL-27Rα (23), and IL-27 deficiency is associated with increased M2 macrophage polarization after respiratory viral infection (24). Relevant to kidney disease, the loss of the IL-27Rα results in increased tissue damage in mouse models of glomerulonephritis (25, 26), and lower levels of serum IL-27 have been associated with nephritis in patients with systemic lupus erythematosus (SLE) (27). However, other work has shown that IL-27 can have opposing effects in the acute and chronic stages of nephrotoxic serum nephritis (20) and that systemic IL-27 levels are increased in some patients with lupus nephritis (28). While this literature provides evidence that IL-27 influences the immune response in the kidney, it also highlights that a knowledge gap remains about the function of IL-27 in different stages and type of kidney disease. Therefore, the unilateral ureteral obstruction (UUO) model was used to better understand the role of IL-27 in either promoting or limiting the development of kidney pathology.

The studies presented here show that after UUO, IL-27Rα deficiency leads to more severe renal injury and fibrosis associated with an increase in chemokines, M2 macrophages and a population of $CD4^+$ cells that co-produces IL-17 and TNFα. These cytokines can act on primary renal epithelial cells to induce chemokines including CCL2, an effect that is antagonized by IL-27. In IL-27Rα$^{-/-}$ mice, IL-17A blockade abrogates renal injury and decreases CCL2 production. Evidence that these pathways are relevant to clinical disease is suggested by increased levels of IL-27 and IL-17 in the serum of patients and by increased IL-27Rα and IL-17RA mRNA in the tubular epithelial cells of patients with CKD. Together,

these studies identify a role for IL-27 as an endogenous negative regulator of inflammatory pathways that contribute to fibrosis in the kidney during UUO and provide evidence that these pathways are operational in patients with CKD.

MATERIALS AND METHODS

Mice and Experimental Design

IL-27Rα$^{-/-}$ mice were originally provided by Amgen and bred in our facility(29). C57BL/6 mice were ordered from Taconic (Germantown, NY). All mice strains were housed, maintained, and bred under specific pathogen-free conditions at the University of Pennsylvania. For UUO, mice were anesthetized using isoflurane in an induction box, and anesthesia was maintained with a face mask with a 1–2% isoflurane. The surgical site was prepared by shaving the appropriate site, cleaning gross hair and debris, and performing a surgical scrub using chlorhexidine. A suprapubic midline laparotomy was performed to visualize the left ureter. Two ligatures (5–0 prolene) were placed around the mid-section of the left ureter and the ureter was divided between the two ligatures. For sham surgeries, an abdominal incision was made but ligation and division were not performed. The body wall was closed using 5–0 synthetic absorbable sutures and the overlying skin apposed with surgical glue. The mice were observed and allowed to recover in a clean cage with a heating pad beneath for heat support until resuming normal activity. Buprenorphine was given to all mice post-operatively for a duration and frequency consistent with pain anticipated to be associated with specific procedures. Mice were monitored once or twice daily for the first three days following the procedure and then a minimum of three times per week after that time. Animals were monitored to assess for signs of pain or discomfort, including inactivity, poor grooming, or decreased oral intake of food and water. Wounds were assessed for signs of infection including drainage, swelling, or erythema. Animals that exhibited signs of pain received additional analgesics as needed (buprenorphine, 0.1 mg/kg, subcutaneously, q12hrs). IL-17 blockade was performed as follows: 500 ng of anti-mouse IL-17A (BioXCell) were injected intraperitoneally (i.p.) in five IL-27Rα$^{-/-}$ mice on 0, 2, 4, 6, 8, 10, and 12 d.p.o. As a control, a rat IgG2a specific for trinitrophenol was injected i.p. using the same treatment regimen.

Ethics Statement

All experimental procedures with mice were approved by the Institutional Animal Care and Use Committee of the University of Pennsylvania in accordance with guidelines of the Association for Assessment and Accreditation of Laboratory Animal Care. Mice were euthanized by administration of CO_2 for at least five minutes in accordance with these guidelines.

Real-Time Quantitative PCR

Total RNA was purified from lungs using TRIzol (Life Technologies). RNA was reverse transcribed and amplified with specific primers in the presence of Power SYBR Green PCR Master Mixture (Applied Biosystems; Life Technologies). The primers for NGAL, CCL2, CCL4, CCL5, CXCL9, CXCL10, and β-actin were obtained from Quantitect (QIAGEN). Normalization was conducted based on levels of beta-actin.

Cell Preparation and Analysis

Single cell suspensions were generated from mouse kidneys. Mice were perfused with 20mL PBS prior to organ procurement. Kidneys were diced and digested in a solution of 1 mg/ml collagenase A (Roche) and 100 μg/ml DNase (Roche) in complete DMEM for 60 min at 37°C to obtain a single-cell suspension. Red blood cells were lysed using 0.86% ammonium chloride (Sigma). Cells from all tissues were counted, washed in flow cytometry buffer (1% BSA (Sigma), 2mM EDTA (Invitrogen) in PBS) and stained for surface markers. For assessment of cytokine production, T cells were restimulated with PMA and ionomycin plus brefeldin A (BGA) and monensin (Sigma) and stained for surface markers, then fixed with 4% paraformaldehyde for ten minutes prior to intracellular staining for relevant cytokines (30). Cells were blocked with 2.4G2 (BioXCell) and Rat IgG (Invitrogen) before staining with monoclonal antibodies. Samples were acquired using an LSRFortessa flow cytometer (BD Biosciences) and analyzed with FlowJo software (Tree Star, Inc.). Viable cells were identified using the LIVE/DEAD Fixable Aqua Dead Cell Stain Kit for 405nm excitation (Invitrogen). The following mAb against mouse antigens were used for staining: FITC-anti-CD3 (clone 145–2c11), FITC-anti-CD19 (clone 6D5), FITC-anti-NK1.1 (clone PK136), ef780-anti-CD11b (clone M1/70), PerCP-anti-Ly6c (clone HK1.4), Pacific Blue-anti-Ly6G (clone 1A8), ef780-anti-CD3 (clone 145–2c11), PE CF594-anti-CD4 (clone GK1.5), Pacific Blue-anti-CD8α (clone 53–6.7), FITC-anti-Foxp3 (clone 150D/E4), PerCP-anti-IL-17A (clone eBio17B7), AF700-anti-CD45 (clone 30-F11), ef780-anti-CD11c (clone N418), PE-anti-F4/80 (clone BM8), PerCP-anti-CD11b (clone M1/70), APC-anti-CD206 (clone C068C2), PE-anti-CD11a (clone H155–78), PE-Cy7-anti-KLRG1 (clone 2F1), Pacific Blue-anti-MHC class II (clone M5/114.15.2).

Hydroxyproline Assay

Fibrotic kidney tissue was snap frozen and stored at −80°C until ready for use. Tissue was weighed and hydrolyzed by incubating for 20 hours at 95°C in a thermoblock and then centrifuged for 10 min at 13,000 × g. Collagen was then quantified using the Quickzyme hydroxyproline assay kit and plotted by tissue weight.

Histology

After perfusion, kidney tissue was fixed for at least 24 hours in 0.5 ml of 10% neutral-buffered formalin solution. Fixed kidney tissues were embedded in paraffin, and sections were cut using a standard procedure. Deparaffinized sections from fixed kidneys were stained with anti-CD3 (Abcam ab16669, Rb mAb) and anti-F4/80 (CST 70076, Rb mAb), and T cells and macrophages were counted per high-powered field at 20x magnification.

RNA sequencing

For human samples, tubules from 256 patient samples (approximately 50 per group) were microdissected to separate the tubule and glomerulus. Poly(A) purified mRNA was isolated from total RNA, and RNA counts were sequenced. Trimmed reads were aligned to the Gencode human genome and then tested with DESeq2 for differential gene expression. Groups are: Con (no renal disease), CKD (GFR<60), DKD (CKD<60 in diabetics), DM (diabetes with GFR>60), HTN (hypertension with GFR>60) (31–33).

For single cell RNA sequencing in mouse kidney tissue, single cell suspensions were prepared from 6 control and 2 UUO kidneys with detailed methods as previously described (34). Briefly, cDNA was barcoded and synthesized using Gel Bead-In-EMulsions (GEMs). The GEMs were incubated with enzymes to produce full length cDNA, which was then amplified by PCR to general libraries. Qualitative analysis was performed using Agilent Bioanalyzer High Sensitivity assay. The cDNA libraries were constructed using the 10x Chromium™ Single cell 3' Library Kit according to the manufacturer's original protocol. Briefly, after the cDNA amplification, enzymatic fragmentation and size selection were performed using SPRI select reagent (Beckman Coulter, Cat# B23317) to optimize the cDNA size. Once the gene-cell data matrix was generated, poor quality cells were excluded, such as cells with <200 or >3,000 unique genes expressed genes (as they are potentially cell duplets). Only genes expressed in 10 or more cells were used for further analysis. Cells were also discarded if their mitochondrial gene percentages were over 50%, resulting in 16,383 genes across 44,343 cells. The data were natural log transformed and normalized for scaling the sequencing depth to a total of 1e4 molecules per cell, followed by regressing-out the number of UMI using Seurat package. Batch effect was corrected by using removeBatchEffect function of edgeR.

Serum ELISAs

Serum samples were obtained from the Penn Medicine BioBank (PMBB). IRB approval was obtained through the University of Pennsylvania, and de-identified samples were obtained using the following inclusion criteria (ICD-10 codes noted): Hypertensive CKD I12.0, I12.9, I13; CKD N18.2 (stage 2), N18.3 (stage 3), N18.4 (stage 4), N18.5, N18.6 (ESRD); Proteinuria R80.9; Requiring chronic dialysis Z99.2; Hypertension I10; Diabetic nephropathy E08.21, E09.21, E10.21, E11.21, E13.21, E11.29, E10.29, E13.29, E08.22, E08.29, E09.22, E09.29, E10.22, E11.22, E13.22; Kidney transplant candidate Z76.82; Kidney transplant failure T86.12; Eligible for kidney transplant, but patient declines Z53.20; Elevated serum creatinine R79.89; Kidney disease N28.9; Kidney fibrosis N26.9; Kidney function test abnormal R94.4; Kidney scarring N28.89; Anemia due to CKD Z86.2; Secondary hyperparathyroidism N25.81, Z86.39; Status post biopsy of kidney Z98.890; Interstitial fibrosis present on biopsy of kidney N26.9. Exclusion criteria included: Kidney malignancy C64.9; Kidney mass N28.89; Kidney neoplasm D49.519; Acute kidney injury N17.9; Polycystic kidney disease Q61.3; Glomerulonephritis, acute N00.9, N01.9, N00.8. Control samples were those in which the following diagnoses were excluded: Hypertensive CKD I12.0, I12.9, I13; CKD N18.2 (stage 2), N18.3 (stage 3), N18.4 (stage 4), N18.5, N18.6 (ESRD); Proteinuria R80.9; Requiring chronic dialysis Z99.2; Hypertension I10; Diabetic nephropathy E08.21, E09.21, E10.21, E11.21, E13.21, E11.29, E10.29, E13.29, E08.22, E08.29, E09.22, E09.29, E10.22, E11.22, E13.22. Serum ELISA was performed using BioLegend Legend Max ELISA Kit of the Human IL-27 Heterodimer.

Statistics

Bar graphs and scatter plots were plotted as means with the SEM in Prism 5 software (GraphPad). All statistical analysis was performed using an unpaired Student *t* test with the exception of histologic evaluations, which were analyzed using the Mann-Whitney U test.

RESULTS

IL-27Rα expression increases on immune cells after UUO injury, and IL-27Rα deficiency leads to increased renal damage after ureteral obstruction

To study the effects of IL-27 on fibrogenic immune pathways in the kidney, renal fibrosis was induced by ureteral obstruction, and disease progression was compared. Surgical groups were sham (abdominal incision only) versus UUO. Control (contralateral, unobstructed) kidneys were compared to sham to assess for effects of circulating immune cells in the post-surgical mouse. Across multiple experiments, no significant differences between sham and control groups were observed in levels of pathology and increases in cytokines (data not shown). UUO injury leads to a chronic tubulointerstitial nephritis, characterized by tubular atrophy, interstitial fibrosis, and inflammatory infiltrate (35). To assess the expression levels of IL-27 and IL-27ra mRNA in the injured kidney, WT control and fibrotic kidneys at 7 days post obstruction (dpo) were used for single cell RNA. Consistent with previously published data, innate cells were the primary sources of IL-27p28 and EBi3(36), and there were basal levels of transcripts in these populations isolated from normal or UUO kidneys (Fig 1A). However, while a number of immune cells had some baseline expression of IL-27ra mRNA, plasmacytoid dendritic cells (pDCs) and $CD4^+$ T cell subsets had the largest increase in expression after UUO (Fig 1A).

To investigate the role of IL-27 signaling in obstructive renal injury, WT and IL-27Rα$^{-/-}$ mice underwent UUO, and kidneys were evaluated by histology for damage. At 7 dpo these mice exhibited modest renal damage without evidence of necrotic changes, neutrophilic inflammation, and extensive tubular loss. Parenchymal atrophy was mild, generally involving less than 50% of the examined section, and accompanied by features of tubular regeneration. Slight interstitial fibrosis was invariably associated with the atrophic parenchymal changes. In addition, few scattered infiltrates of mononuclear cells were frequently observed in the interstitium of the affected regions. Based on previously published results immune cell infiltration is best evaluated at 14 dpo; therefore, this time point was chosen for analyses for immune cell analysis (35). In WT kidneys, UUO led to an expected increase in fibrosis as measured by collagen levels (Fig 1B) in association with an increase in neutrophil gelatinase-associated lipocalin (NGAL), a marker of renal injury (37) (Fig 1C). In the obstructed kidneys of IL-27Rα$^{-/-}$ mice, collagen deposition and NGAL mRNA were elevated over WT controls (Fig 1B–C).

IL-27Rα deficiency is associated with increased macrophage infiltration and M2 macrophage polarization in fibrotic kidneys

Given the increased expression of IL-27ra mRNA on pDCs after UUO (characterized by transcripts for Ly6d, Cox6a2, CD209d, Bcl11a, Klkb27, Spib, CD300c, Fcrla, and Atp2a1 mRNA), $CD11b^+$/MHC class 2^+ dendritic cells were identified in fibrotic kidneys using flow cytometry and further subset into classical DCs (cDCs) and pDCs using the markers CD103 and CX3CR1 as previously described (38). At 14 dpo there was no difference in frequency of either DC subset in the damaged kidneys of WT versus IL-27Rα$^{-/-}$ mice (Fig 2A). The presence of macrophages is associated with kidney fibrosis (39), and consistent with this there were higher numbers of $F4/80^+$ macrophages in the kidneys of IL-27Rα$^{-/-}$ mice when

compared to WT after UUO (Fig 2B). Further analysis of these cells in the kidneys of both WT and IL-27Rα$^{-/-}$ mice revealed a subset of CD64^{+} F4/80^{+} macrophages that expressed CD206 (the mannose receptor and a marker of M2 polarization) (7, 8, 40), which was increased in the absence of the IL-27Rα (Fig 2C). The use of immunohistochemistry (IHC) to visualize these macrophages, based on expression of CD68 and the M2 marker Ym1, showed that in IL-27Rα$^{-/-}$ mice with UUO there were prominent infiltrates of these cells in the tubulointerstitium (Fig 2C). These data sets establish that while the phenotype of DCs in fibrotic kidneys is not affected by IL-27 signaling, the enhanced renal fibrosis observed in IL-27Rα$^{-/-}$ deficient mice is associated with increased recruitment of macrophages and polarization to the M2 phenotype.

CD4^{+} T cell responses are enhanced in the fibrotic kidneys of IL-27Rα$^{-/-}$ mice

Previous studies have established that T cells contribute to the development of fibrosis in the kidney after UUO injury, but little is known about the characteristics of CD4^{+} T cells associated with these events(10). Both WT and IL-27Rα$^{-/-}$ mice had an increase in CD3^{+} T cell clustering around the tubules in the fibrotic kidneys (Fig 3A). However, IL-27Rα deficiency resulted in higher numbers of T cells in fibrotic kidneys (Fig 3A). CD4^{+} T cells promote fibrosis in the kidney after UUO(10); therefore, the CD4^{+} T cells were assessed for expression of activation markers at 14 dpo. T cells typically express basal levels of CD11a, a component of the adhesion molecule leukocyte function associated antigen-1 molecule (LFA-1), and the expression of high levels of CD11a (CD11a^{hi}) serves as a marker of antigen experience (41, 42). Analysis of CD4^{+} T cells in both WT and IL-27Rα$^{-/-}$ mouse kidneys revealed a bimodal distribution of CD11a^{+} and CD11a^{hi} cells (Fig 3B), but in the IL-27Rα$^{-/-}$ mice, the MFI of CD11a was higher in CD4^{+} T cells (Fig 3B). A comparison of the phenotypes of the CD11a^{hi} cells based on the expression of the activation markers CD44, KLRG1, and CD69 revealed that expression of all three of these surface markers was elevated in IL-27 deficiency (Fig 3C–E). As these differences were not observed in the non-fibrotic control kidneys, these data indicate that the protective effects of IL-27 operate at the level of the damaged tissue.

To determine if the loss of IL-27 signaling affects the function of CD4^{+} T cells in the injured kidneys, cytokine production by these cells was assessed in WT and IL-27Rα$^{-/-}$ mice. No IL-2, IFN-γ, GMCSF, IL-13, or IL-9 was detected in these samples at 14 dpo (supplemental figure 2). While low levels of TNFα and IL-17A were produced by WT CD4^{+} T cells, both cytokines were produced at higher levels by the IL-27Rα$^{-/-}$ CD4^{+} T cells, and a population that co-expressed them was also observed (Fig 3F–G). On average, over three experiments, there were around 300–400 Th17 cells in WT UUO kidney sections and 1000–3000 Th17 cells in IL-27Rα$^{-/-}$ kidney sections. These T cell responses were specific to the affected kidney and were not observed in the spleen or draining lymph nodes (data not shown). Of note, γδ T cells were not found to express IL-27ra, and IL-17 production was not different between these cells in WT and IL-27Rα$^{-/-}$ mice (supplemental fig 1).

IL-27Rα deficiency is associated with increased chemokine expression after UUO

IL-17A and TNFα can induced the production of chemokines such as CCL2, CXCL10, and CCL5 (43–45), and these cytokines act in synergy on nonhematopoietic cells to enhance

chemokine production (46, 47). Given the increased immune cell infiltration detected in the fibrotic kidneys of IL-27Rα$^{-/-}$ mice, RT-PCR was used to compare levels of CXCL10, CCL5, CCL4, and CCL2 mRNA in the fibrotic kidneys of WT versus IL-27Rα$^{-/-}$ mice. In damaged WT kidneys, fibrosis was associated with a modest increase in the levels of these chemokines; however, after UUO IL-27Rα$^{-/-}$ mice had a marked increase in the levels of all chemokines examined (Fig 4A–D). Because the ability of IL-17A to promote CCL2 contributes to immune cell recruitment in other systems (48, 49), primary renal epithelial cells were cultured with IL-17 and TNFα, and levels of chemokine mRNA were measured (Fig 4E). In these studies, CXCL10, CCL4, and CCL5 did not respond synergistically to IL-17A and TNFα (data not shown). These two cytokines did act synergistically to induce CCL2 mRNA, and the addition of IL-27 limited its production (Fig 4E). Together, these data highlight that increased chemokine production and most notably elevated CCL2 correlated with enhanced Th17 responses and the increased immune cell infiltration and damage seen in IL-27Rα$^{-/-}$ mice.

IL-17 blockade ameliorates renal fibrosis after UUO in IL-27Rα$^{-/-}$ mice

Given the emerging evidence that Th17 cells are important mediators of renal disease and the elevated Th17 responses detected in the IL-27Rα$^{-/-}$ mice after UUO, experiments were performed to determine whether IL-17A contributes to the enhanced renal injury in IL-27Rα$^{-/-}$ mice. Therefore, a monoclonal antibody against IL-17A or isotype control was administered to IL-27Rα$^{-/-}$ at 0, 2, 4, 6, 8, 10, and 12 dpo, and tissues were analyzed at 13 dpo. IL-17A blockade did not alter levels of collagen deposition (Fig 5A) but did result in a marked decrease in NGAL mRNA (Fig 5B). In addition, while IL-17A blockade did not alter the levels of CCL4, CCL5, or CXCL9 (data not shown), this treatment did lead to a decrease in CCL2 mRNA (Fig 5C). Furthermore, while anti-IL-17A did not decrease macrophage recruitment or M2 macrophage frequency in the kidney (Fig 5D) there was a significant decrease in CD3^{+} T cells in the injured kidneys of IL-27Rα$^{-/-}$ mice (Fig 5E). These findings indicate that in the absence of the IL-27Rα, IL-17A contributes to the increased renal pathology by promoting CCL2 and T cell recruitment. In addition, that IL-17 blockade did not affect the infiltration and polarization of M2 macrophages suggests that the protective effects of IL-27 in UUO are not solely through the ability to block IL-17A production.

IL-27 and IL-17A are associated with progressive renal damage in patients with CKD

The cytokines IL-6 and IL-10 have been detected at higher levels in the blood of patients with kidney injury any may be used to predict disease trajectory in AKI and CKD (50). Therefore, in an effort to determine if CKD was associated with changes in IL-27 or IL-17A, serum from patients with normal renal function and those with CKD stage 3 or greater were assayed for levels of these cytokines by ELISA. Most patients with CKD had isolated increases in either cytokine with about 25% showing increases in both IL-17A and IL-27 (Fig 6A). These data show that IL-27 and IL-17A are produced during CKD, but the presence of elevated IL-17A, IL-27, or both cytokines did not correlate with diagnoses of diabetes, hypertension, or degree of CKD. Next, renal tubular epithelial cells were microdissected from patients with normal renal function (Con), CKD (glomerular filtration rate less than 60 ml/min), diabetic kidney disease (DKD), diabetes without kidney disease

(DM), and hypertension without kidney disease (HTN). IL-27RA and IL-17RA mRNA levels were compared across groups by estimated glomerular filtration rate (eGFR), and degree of fibrosis. Analysis of these samples revealed that when compared to controls with normal renal function there was increased expression of the IL-27Rα and IL-17RA on the tubular epithelium of patients with enhanced renal fibrosis (Fig 6B). These data indicate that IL-27 and IL-17 and their receptors are detectable in patient samples and that the regulatory pathways associated with these cytokines are relevant to a subset of human kidney disease.

DISCUSSION

Several studies have previously established a role for IL-27 in inflammatory injury in the kidney (25, 51); however, it has been associated with protective and pathologic functions (20, 51), which illustrates the context-dependent effects of endogenous IL-27. The data presented here highlight a novel role for IL-27 in limiting inflammatory renal fibrosis. Thus, following UUO injury IL-27Rα$^{-/-}$ mice had increased renal fibrosis and that this was associated with the presence of polyfunctional Th17 cells that co-expressed TNFα. Heterogeneous CD4^{+} T cell responses, defined here as CD4^{+} T cells that produce cytokines from distinct lineages (for example, IL-17/IFNγ, IL-13/IFNγ), have been identified as pathologic mediators of disease (52–55). These dysregulated immune pathways were associated with an increase in the chemokine CCL2 and a higher frequency of M2 macrophages. CCL2, also known as monocyte chemoattractant protein-1 (MCP-1), can be induced by IL-17A and plays an important role in multiple forms of kidney injury, that include diabetic nephropathy, glomerulonephritis, and glomerulosclerosis (56). Thus, in this model of kidney damage, endogenous IL-27 is associated with the suppression of conventional and heterogeneous Th17 responses in the kidney as well as their downstream sequelae such as renal fibrosis.

The ability of IL-27 to antagonize Th17 cells and decrease immune-mediated pathology has been described in multiple models of inflammation (21, 22, 57). Th17 cells have broad relevance in the kidney as they can precipitate renal inflammation in autoimmune disease, salt-mediated renal injury, and sepsis (12, 47, 58). Therefore, they represent an important potential target for preventative therapy, and the impact of IL-17A blockade shown here supports this idea. Relevant to other models of kidney disease, IL-27 deficiency corresponds to heightened Th17 responses and increased immune pathology in acute glomerulonephritis (25), whereas the studies presented here associated IL-27 with the ability to limit fibrosis. Interestingly, other studies have shown that IL-17A$^{-/-}$ mice are protected against UUO injury(14) while IL-17RA$^{-/-}$ mice had exacerbated fibrosis after UUO(59). This suggests that some of the other members in the IL-17 cytokine family (IL-17B-E) may have protective effects in kidney fibrosis and merits further study. In a model of atherosclerosis, mice genetically predisposed to develop fibrosis of the arterial wall (Ldlr$^{-/-}$) developed worse disease after receiving IL-27Rα$^{-/-}$ bone marrow (60). In this experimental system, IL-27Rα$^{-/-}$ CD4^{+} T cells at the site of inflammation produced higher levels of IL-17 and TNFα, which corresponded with increased CCL2 production at the aorta (60). One link that has emerged in these data is that IL-17 and TNFα act directly on epithelial cells to upregulate CCL2. These observations highlight the potential for chronic damage in long-term Th17-mediated kidney disease and fit with clinical data that IL-17 contributes to the

pathogenesis of other chronic diseases such as psoriasis, atherosclerosis, and asthma (61–63).

One of the prominent features of the pathology that developed in the absence of IL-27 was the presence of a major population of M2 macrophages. It has been reported that M2 macrophages express the IL-27Rα, and IL-27 can limit M2 macrophage polarization (23, 24). M2 macrophages have been associated with increased renal immunopathology (4, 64), but it is unclear how they affect various stages of injury. For example, some subsets of M2 macrophages may be protective against acute renal injury, while others are considered to be profibrotic (65). Further characterization and functional analysis of the macrophage subsets that emerge during acute renal damage or in the setting of IL-27 deficiency is warranted to better understand how these cells contribute to renal pathology and whether their activities are beneficial or detrimental.

From a translational perspective, little is known about whether changes in IL-27, IL-17 and/or their relative receptors are associated with kidney disease. Circulating IL-27 is present at very low levels in normal serum, and changes in serum IL-27 concentration have been reported in patients with lupus nephritis (28, 66). However, in some cases lower levels have been associated with increased disease pathology (27, 66). Th17 cells infiltrate fibrotic kidney tissue in transplant recipients (67), and gene polymorphisms in IL-17 and the IL-27R are associated with end stage renal disease (ESRD) (68). The elevated serum levels of IL-27 and IL-17 in a subset of patients with CKD indicate that these cytokines are relevant in the progression of renal fibrosis, while the data with the renal tubular epithelial cells highlight that these specialized epithelial cells should be considered as major targets for both IL-27 and IL-17 during CKD. Thus, the studies presented here using a murine model highlight a role for IL-27 in limiting profibrotic inflammatory pathways in the kidney but also raise the potential for IL-27 to be used as a biomarker and/or a therapeutic agent in CKD patients.

Supplementary Material

Refer to Web version on PubMed Central for supplementary material.

ACKNOWLEDGEMENTS

The authors would like to thank Cristian Perez and the Penn Medicine BioBank (PMBB) for sample preparation and delivery.

Funding relevant to this work

GMC: ASN Ben Lipps Research Fellowship, University of Pennsylvania School of Medicine Measey Research Fellowship

CAH: NIH R01 A1041158, NIH R01 AI125563

KS: Grants from Merck, Gilead, Bayer, GSK, BiPi, and Regeneron, NIH R01 DK087635

References

1. 2015 Kidney Disease Statistics for the United States.
2. Wick G, Grundtman C, Mayerl C, Wimpissinger TF, Feichtinger J, Zelger B, Sgonc R, and Wolfram D. 2013 The immunology of fibrosis. Annu Rev Immunol 31: 107–135. [PubMed: 23516981]

3. Kurts C, Panzer U, Anders HJ, and Rees AJ. 2013 The immune system and kidney disease: basic concepts and clinical implications. Nat Rev Immunol 13: 738–753. [PubMed: 24037418]

4. Belliere J, Casemayou A, Ducasse L, Zakaroff-Girard A, Martins F, Iacovoni JS, Guilbeau-Frugier C, Buffin-Meyer B, Pipy B, Chauveau D, Schanstra JP, and Bascands JL. 2015 Specific macrophage subtypes influence the progression of rhabdomyolysis-induced kidney injury. J Am Soc Nephrol 26: 1363–1377. [PubMed: 25270069]

5. Han Y, Ma FY, Tesch GH, Manthey CL, and Nikolic-Paterson DJ. 2013 Role of macrophages in the fibrotic phase of rat crescentic glomerulonephritis. Am J Physiol Renal Physiol 304: F1043–1053. [PubMed: 23408165]

6. Kim MG, Kim SC, Ko YS, Lee HY, Jo SK, and Cho W. 2015 The Role of M2 Macrophages in the Progression of Chronic Kidney Disease following Acute Kidney Injury. PLoS One 10: e0143961. [PubMed: 26630505]

7. Braga TT, Correa-Costa M, Guise YF, Castoldi A, de Oliveira CD, Hyane MI, Cenedeze MA, Teixeira SA, Muscara MN, Perez KR, Cuccovia IM, Pacheco-Silva A, Gonçalves GM, and Camara NO. 2012 MyD88 signaling pathway is involved in renal fibrosis by favoring a TH2 immune response and activating alternative M2 macrophages. Mol Med 18: 1231–1239. [PubMed: 22777483]

8. Toki D, Zhang W, Hor KL, Liuwantara D, Alexander SI, Yi Z, Sharma R, Chapman JR, Nankivell BJ, Murphy B, and O'Connell PJ. 2014 The role of macrophages in the development of human renal allograft fibrosis in the first year after transplantation. Am J Transplant 14: 2126–2136. [PubMed: 25307039]

9. Ascon M, Ascon DB, Liu M, Cheadle C, Sarkar C, Racusen L, Hassoun HT, and Rabb H. 2009 Renal ischemia-reperfusion leads to long term infiltration of activated and effector-memory T lymphocytes. Kidney Int 75: 526–535. [PubMed: 19092796]

10. Liu L, Kou P, Zeng Q, Pei G, Li Y, Liang H, Xu G, and Chen S. 2012 CD4+ T Lymphocytes, especially Th2 cells, contribute to the progress of renal fibrosis. Am J Nephrol 36: 386–396. [PubMed: 23052013]

11. Wynn TA 2004 Fibrotic disease and the T(H)1/T(H)2 paradigm. Nat Rev Immunol 4: 583–594. [PubMed: 15286725]

12. Mehrotra P, Patel JB, Ivancic CM, Collett JA, and Basile DP. 2015 Th-17 cell activation in response to high salt following acute kidney injury is associated with progressive fibrosis and attenuated by AT-1R antagonism. Kidney Int 88: 776–784. [PubMed: 26200947]

13. Park J, Goergen CJ, HogenEsch H, and Kim CH. 2016 Chronically Elevated Levels of Short-Chain Fatty Acids Induce T Cell-Mediated Ureteritis and Hydronephrosis. J Immunol 196: 2388–2400. [PubMed: 26819206]

14. Peng X, Xiao Z, Zhang J, Li Y, Dong Y, and Du J. 2015 IL-17A produced by both γδ T and Th17 cells promotes renal fibrosis via RANTES-mediated leukocyte infiltration after renal obstruction. J Pathol 235: 79–89. [PubMed: 25158055]

15. Marangoni RG, Masui Y, Fang F, Korman B, Lord G, Lee J, Lakota K, Wei J, Scherer PE, Otvos L, Yamauchi T, Kubota N, Kadowaki T, Asano Y, Sato S, Tourtellotte WG, and Varga J. 2017 Adiponectin is an endogenous anti-fibrotic mediator and therapeutic target. Sci Rep 7: 4397. [PubMed: 28667272]

16. Ariel A, and Timor O. 2013 Hanging in the balance: endogenous anti-inflammatory mechanisms in tissue repair and fibrosis. J Pathol 229: 250–263. [PubMed: 23007838]

17. Stumhofer JS, Laurence A, Wilson EH, Huang E, Tato CM, Johnson LM, Villarino AV, Huang Q, Yoshimura A, Sehy D, Saris CJ, O'Shea JJ, Hennighausen L, Ernst M, and Hunter CA. 2006 Interleukin 27 negatively regulates the development of interleukin 17-producing T helper cells during chronic inflammation of the central nervous system. Nat Immunol 7: 937–945. [PubMed: 16906166]

18. Stumhofer JS, Silver JS, Laurence A, Porrett PM, Harris TH, Turka LA, Ernst M, Saris CJ, O'Shea JJ, and Hunter CA. 2007 Interleukins 27 and 6 induce STAT3-mediated T cell production of interleukin 10. Nat Immunol 8: 1363–1371. [PubMed: 17994025]

19. Fitzgerald DC, Zhang GX, El-Behi M, Fonseca-Kelly Z, Li H, Yu S, Saris CJ, Gran B, Ciric B, and Rostami A. 2007 Suppression of autoimmune inflammation of the central nervous system by

interleukin 10 secreted by interleukin 27-stimulated T cells. Nat Immunol 8: 1372–1379. [PubMed: 17994023]

20. Summers SA, Phoon RK, Ooi JD, Holdsworth SR, and Kitching AR. 2011 The IL-27 receptor has biphasic effects in crescentic glomerulonephritis mediated through Th1 responses. Am J Pathol 178: 580–590. [PubMed: 21281790]
21. Moon SJ, Park JS, Heo YJ, Kang CM, Kim EK, Lim MA, Ryu JG, Park SJ, Park KS, Sung YC, Park SH, Kim HY, Min JK, and Cho ML. 2013 In vivo action of IL-27: reciprocal regulation of Th17 and Treg cells in collagen-induced arthritis. Exp Mol Med 45: e46. [PubMed: 24091748]
22. Liu FD, Kenngott EE, Schröter MF, Kühl A, Jennrich S, Watzlawick R, Hoffmann U, Wolff T, Norley S, Scheffold A, Stumhofer JS, Saris CJ, Schwab JM, Hunter CA, Debes GF, and Hamann A. 2014 Timed action of IL-27 protects from immunopathology while preserving defense in influenza. PLoS Pathog 10: e1004110. [PubMed: 24809349]
23. Rückerl D, Hessmann M, Yoshimoto T, Ehlers S, and Hölscher C. 2006 Alternatively activated macrophages express the IL-27 receptor alpha chain WSX-1. Immunobiology 211: 427–436. [PubMed: 16920482]
24. Muallem G, Wagage S, Sun Y, DeLong J, Valenzuela A, Christian D, Pritchard G, Fang Q, Buza E, Jain D, Elloso M, Lopez C, and Hunter C. IL-27 Limits Type 2 Immunopathology Following Parainfluenza Virus Infection.
25. Pawaria S, Ramani K, Maers K, Liu Y, Kane LP, Levesque MC, and Biswas PS. 2014 Complement Component C5a Permits the Coexistence of Pathogenic Th17 Cells and Type I IFN in Lupus. J Immunol.
26. Sugiyama N, Nakashima H, Yoshimura T, Sadanaga A, Shimizu S, Masutani K, Igawa T, Akahoshi M, Miyake K, Takeda A, Yoshimura A, Hamano S, and Yoshida H. 2008 Amelioration of human lupus-like phenotypes in MRL/lpr mice by overexpression of interleukin 27 receptor alpha (WSX-1). Ann Rheum Dis 67: 1461–1467. [PubMed: 18094002]
27. Li TT, Zhang T, Chen GM, Zhu QQ, Tao JH, Pan HF, and Ye DQ. 2010 Low level of serum interleukin 27 in patients with systemic lupus erythematosus. J Investig Med 58: 737–739.
28. Xia L, Li B, Shen H, and Lu J. 2015 Interleukin-27 and interleukin-23 in patients with systemic lupus erythematosus: possible role in lupus nephritis. Scand J Rheumatol: 1–6. [PubMed: 26303149]
29. Villarino A, Hibbert L, Lieberman L, Wilson E, Mak T, Yoshida H, Kastelein RA, Saris C, and Hunter CA. 2003 The IL-27R (WSX-1) is required to suppress T cell hyperactivity during infection. Immunity 19: 645–655. [PubMed: 14614852]
30. Candolfi E, Hunter CA, and Remington JS. 1995 Roles of gamma interferon and other cytokines in suppression of the spleen cell proliferative response to concanavalin A and toxoplasma antigen during acute toxoplasmosis. Infect Immun 63: 751–756. [PubMed: 7868243]
31. Beckerman P, Qiu C, Park J, Ledo N, Ko YA, Park AD, Han SY, Choi P, Palmer M, and Susztak K. 2017 Human Kidney Tubule-Specific Gene Expression Based Dissection of Chronic Kidney Disease Traits. EBioMedicine 24: 267–276. [PubMed: 28970079]
32. Qiu C, and Susztak K. GSE115098 (https://www.ncbi.nlm.nih.gov/geo/query/acc.cgi?acc=GSE115098).
33. Qiu C, Huang S, Park J, Park Y, Ko YA, Seasock MJ, Bryer JS, Xu XX, Song WC, Palmer M, Hill J, Guarnieri P, Hawkins J, Boustany-Kari CM, Pullen SS, Brown CD, and Susztak K. 2018 Renal compartment-specific genetic variation analyses identify new pathways in chronic kidney disease. Nat Med 24: 1721–1731. [PubMed: 30275566]
34. Park J, Shrestha R, Qiu C, Kondo A, Huang S, Werth M, Li M, Barasch J, and Susztak K. 2018 Single-cell transcriptomics of the mouse kidney reveals potential cellular targets of kidney disease. Science.
35. Truong LD, Gaber L, and Eknoyan G. 2011 Obstructive uropathy. Contrib Nephrol 169: 311–326. [PubMed: 21252529]
36. Yoshida H, and Hunter CA. 2015 The immunobiology of interleukin-27. Annu Rev Immunol 33: 417–443. [PubMed: 25861977]
37. Mori K, and Nakao K. 2007 Neutrophil gelatinase-associated lipocalin as the real-time indicator of active kidney damage. Kidney Int 71: 967–970. [PubMed: 17342180]

38. Merad M, Sathe P, Helft J, Miller J, and Mortha A. 2013 The dendritic cell lineage: ontogeny and function of dendritic cells and their subsets in the steady state and the inflamed setting. Annu Rev Immunol 31: 563–604. [PubMed: 23516985]

39. Chevalier RL, Forbes MS, and Thornhill BA. 2009 Ureteral obstruction as a model of renal interstitial fibrosis and obstructive nephropathy. Kidney Int 75: 1145–1152. [PubMed: 19340094]

40. Shiraishi M, Shintani Y, Ishida H, Saba R, Yamaguchi A, Adachi H, Yashiro K, and Suzuki K. 2016 Alternatively activated macrophages determine repair of the infarcted adult murine heart. J Clin Invest 126: 2151–2166. [PubMed: 27140396]

41. Dupont CD, Christian DA, Selleck EM, Pepper M, Leney-Greene M, Harms Pritchard G, Koshy AA, Wagage S, Reuter MA, Sibley LD, Betts MR, and Hunter CA. 2014 Parasite fate and involvement of infected cells in the induction of CD4+ and CD8+ T cell responses to Toxoplasma gondii. PLoS Pathog 10: e1004047. [PubMed: 24722202]

42. Rai D, Pham NL, Harty JT, and Badovinac VP. 2009 Tracking the total CD8 T cell response to infection reveals substantial discordance in magnitude and kinetics between inbred and outbred hosts. J Immunol 183: 7672–7681. [PubMed: 19933864]

43. Park H, Li Z, Yang XO, Chang SH, Nurieva R, Wang YH, Wang Y, Hood L, Zhu Z, Tian Q, and Dong C. 2005 A distinct lineage of CD4 T cells regulates tissue inflammation by producing interleukin 17. Nat Immunol 6: 1133–1141. [PubMed: 16200068]

44. Erdmann H, Behrends J, Ritter K, Holscher A, Volz J, Rosenkrands I, and Holscher C. 2018 The increased protection and pathology in Mycobacterium tuberculosis-infected IL-27R-alpha-deficient mice is supported by IL-17A and is associated with the IL-17A-induced expansion of multifunctional T cells. Mucosal Immunol.

45. Kovacic JC, Gupta R, Lee AC, Ma M, Fang F, Tolbert CN, Walts AD, Beltran LE, San H, Chen G, St Hilaire C, and Boehm M. 2010 Stat3-dependent acute Rantes production in vascular smooth muscle cells modulates inflammation following arterial injury in mice. J Clin Invest 120: 303–314. [PubMed: 20038813]

46. Amara S, Lopez K, Banan B, Brown SK, Whalen M, Myles E, Ivy MT, Johnson T, Schey KL, and Tiriveedhi V. 2015 Synergistic effect of pro-inflammatory TNFα and IL-17 in periostin mediated collagen deposition: potential role in liver fibrosis. Mol Immunol 64: 26–35. [PubMed: 25467797]

47. Ramani K, and Biswas PS. 2016 Interleukin 17 signaling drives Type I Interferon induced proliferative crescentic glomerulonephritis in lupus-prone mice. Clin Immunol 162: 31–36. [PubMed: 26556529]

48. Shahrara S, Pickens SR, Mandelin AM, Karpus WJ, Huang Q, Kolls JK, and Pope RM. 2010 IL-17-mediated monocyte migration occurs partially through CC chemokine ligand 2/monocyte chemoattractant protein-1 induction. J Immunol 184: 4479–4487. [PubMed: 20228199]

49. McGeachy MJ, Bak-Jensen KS, Chen Y, Tato CM, Blumenschein W, McClanahan T, and Cua DJ. 2007 TGF-beta and IL-6 drive the production of IL-17 and IL-10 by T cells and restrain T(H)-17 cell-mediated pathology. Nat Immunol 8: 1390–1397. [PubMed: 17994024]

50. Zhang WR, Garg AX, Coca SG, Devereaux PJ, Eikelboom J, Kavsak P, McArthur E, Thiessen-Philbrook H, Shortt C, Shlipak M, Whitlock R, Parikh CR, and Consortium T-A. 2015 Plasma IL-6 and IL-10 Concentrations Predict AKI and Long-Term Mortality in Adults after Cardiac Surgery. J Am Soc Nephrol.

51. Igawa T, Nakashima H, Sadanaga A, Masutani K, Miyake K, Shimizu S, Takeda A, Hamano S, and Yoshida H. 2009 Deficiency in EBV-induced gene 3 (EBI3) in MRL/lpr mice results in pathological alteration of autoimmune glomerulonephritis and sialadenitis. Mod Rheumatol 19: 33–41. [PubMed: 18779924]

52. Wang YH, Voo KS, Liu B, Chen CY, Uygungil B, Spoede W, Bernstein JA, Huston DP, and Liu YJ. 2010 A novel subset of CD4(+) T(H)2 memory/effector cells that produce inflammatory IL-17 cytokine and promote the exacerbation of chronic allergic asthma. J Exp Med 207: 2479–2491. [PubMed: 20921287]

53. Zhu J, and Paul WE. 2010 Heterogeneity and plasticity of T helper cells. Cell Res 20: 4–12. [PubMed: 20010916]

54. Becattini S, Latorre D, Mele F, Foglierini M, De Gregorio C, Cassotta A, Fernandez B, Kelderman S, Schumacher TN, Corti D, Lanzavecchia A, and Sallusto F. 2015 T cell immunity. Functional

heterogeneity of human memory CD4+ T cell clones primed by pathogens or vaccines. Science 347: 400–406. [PubMed: 25477212]

55. Sallusto F, and Lanzavecchia A. 2009 Heterogeneity of CD4+ memory T cells: functional modules for tailored immunity. Eur J Immunol 39: 2076–2082. [PubMed: 19672903]
56. Haller H, Bertram A, Nadrowitz F, and Menne J. 2016 Monocyte chemoattractant protein-1 and the kidney. Curr Opin Nephrol Hypertens 25: 42–49. [PubMed: 26625862]
57. Hirahara K, Ghoreschi K, Yang XP, Takahashi H, Laurence A, Vahedi G, Sciumè G, Hall AO, Dupont CD, Francisco LM, Chen Q, Tanaka M, Kanno Y, Sun HW, Sharpe AH, Hunter CA, and O'Shea JJ. 2012 Interleukin-27 priming of T cells controls IL-17 production in trans via induction of the ligand PD-L1. Immunity 36: 1017–1030. [PubMed: 22726954]
58. Maravitsa P, Adamopoulou M, Pistiki A, Netea MG, Louis K, and Giamarellos-Bourboulis EJ. 2016 Systemic over-release of interleukin-17 in acute kidney injury after septic shock: Clinical and experimental evidence. Immunol Lett 178: 68–76. [PubMed: 27515003]
59. Ramani K, Tan RJ, Zhou D, Coleman BM, Jawale CV, Liu Y, and Biswas PS. 2018 IL-17 Receptor Signaling Negatively Regulates the Development of Tubulointerstitial Fibrosis in the Kidney. Mediators Inflamm 2018: 5103672. [PubMed: 30405320]
60. Koltsova EK, Kim G, Lloyd KM, Saris CJ, von Vietinghoff S, Kronenberg M, and Ley K. 2012 Interleukin-27 receptor limits atherosclerosis in Ldlr−/− mice. Circ Res 111: 1274–1285. [PubMed: 22927332]
61. Mansouri M, Mansouri P, Raze AA, and Jadali Z. 2018 The potential role of Th17 lymphocytes in patients with psoriasis. An Bras Dermatol 93: 63–66. [PubMed: 29641699]
62. Brauner S, Jiang X, Thorlacius GE, Lundberg AM, Ostberg T, Yan ZQ, Kuchroo VK, Hansson GK, and Wahren-Herlenius M. 2018 Augmented Th17 differentiation in Trim21 deficiency promotes a stable phenotype of atherosclerotic plaques with high collagen content. Cardiovasc Res 114: 158–167. [PubMed: 29016728]
63. Hatta M, Surachmanto EE, Islam AA, and Wahid S. 2017 Expression of mRNA IL-17F and sIL-17F in atopic asthma patients. BMC Res Notes 10: 202. [PubMed: 28606156]
64. Guiteras R, Flaquer M, and Cruzado JM. 2016 Macrophage in chronic kidney disease. Clin Kidney J 9: 765–771. [PubMed: 27994852]
65. Zhang MZ, Wang X, Wang Y, Niu A, Wang S, Zou C, and Harris RC. 2017 IL-4/IL-13-mediated polarization of renal macrophages/dendritic cells to an M2a phenotype is essential for recovery from acute kidney injury. Kidney Int 91: 375–386. [PubMed: 27745702]
66. Duarte AL, Dantas AT, de Ataíde Mariz H, dos Santos FA, da Silva JC, da Rocha LF, Galdino SL, and da Rocha Pitta M. Galdino. 2013 Decreased serum interleukin 27 in Brazilian systemic lupus erythematosus patients. Mol Biol Rep 40: 4889–4892. [PubMed: 23645091]
67. Deteix C, Attuil-Audenis V, Duthey A, Patey N, McGregor B, Dubois V, Caligiuri G, Graff-Dubois S, Morelon E, and Thaunat O. 2010 Intragraft Th17 infiltrate promotes lymphoid neogenesis and hastens clinical chronic rejection. J Immunol 184: 5344–5351. [PubMed: 20357253]
68. Kim YG, Kim EY, Ihm CG, Lee TW, Lee SH, Jeong KH, Moon JY, Chung JH, and Kim YH. 2012 Gene polymorphisms of interleukin-17 and interleukin-17 receptor are associated with end-stage kidney disease. Am J Nephrol 36: 472–477. [PubMed: 23147652]

Key points:

- Th17 cells are associated with renal dysfunction and IL-27 suppresses these cells.
- IL-27R limits renal fibrosis after unilateral ureteral obstruction (UUO).

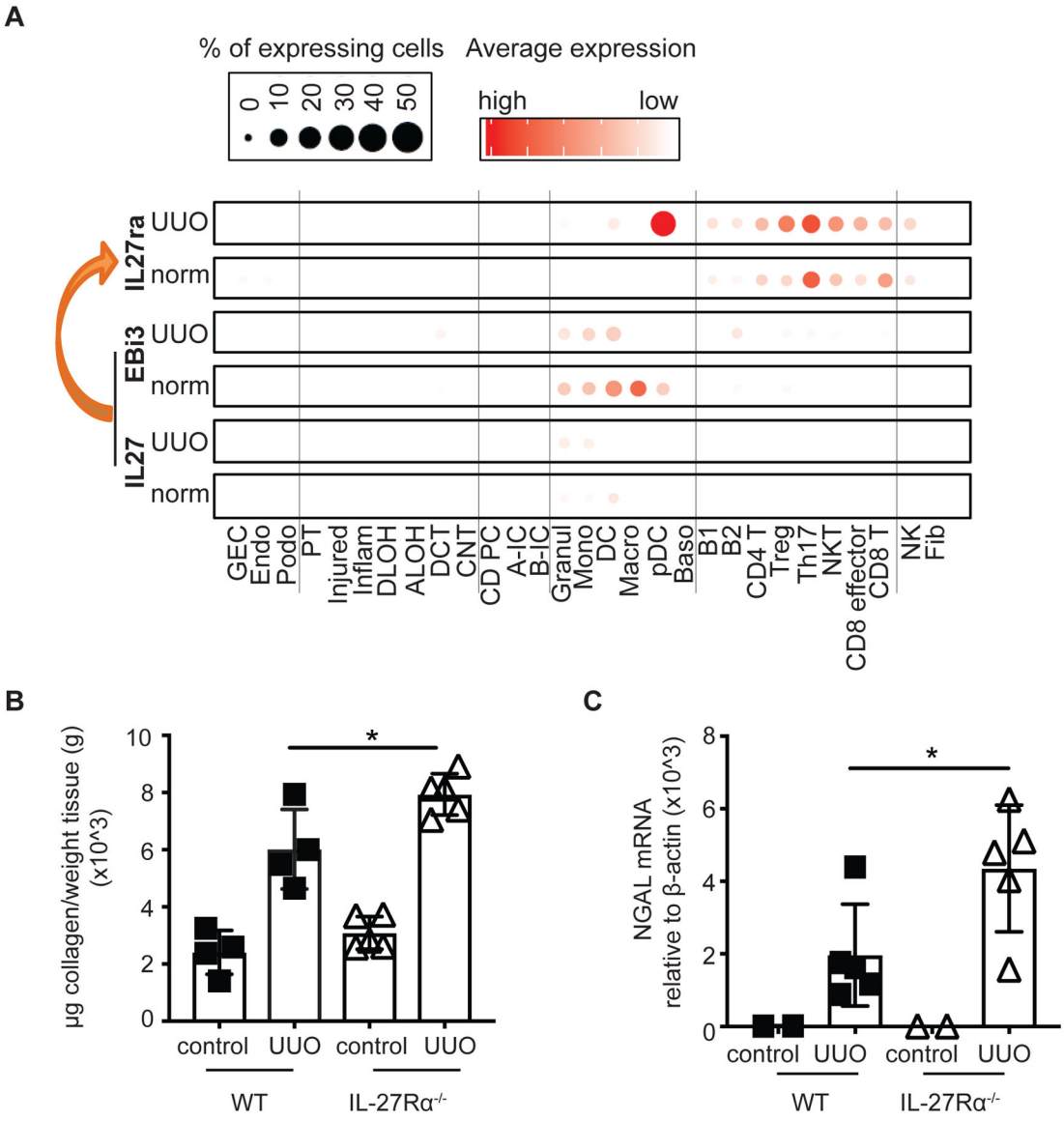

Figure 1:

(A) Single cell RNA sequencing was performed on cells extracted from WT kidneys and %expression plotted for IL-27 and IL-27ra. (B) Collagen content by tissue weight 13 dpo in WT and IL-27R$^{-/-}$ kidneys as indicated. (C) RT-PCR of NGAL mRNA normalized to B-actin in control and fibrotic kidneys as indicated (14 dpo). * p<0.05, ** p<0.005, **** p<0.0005

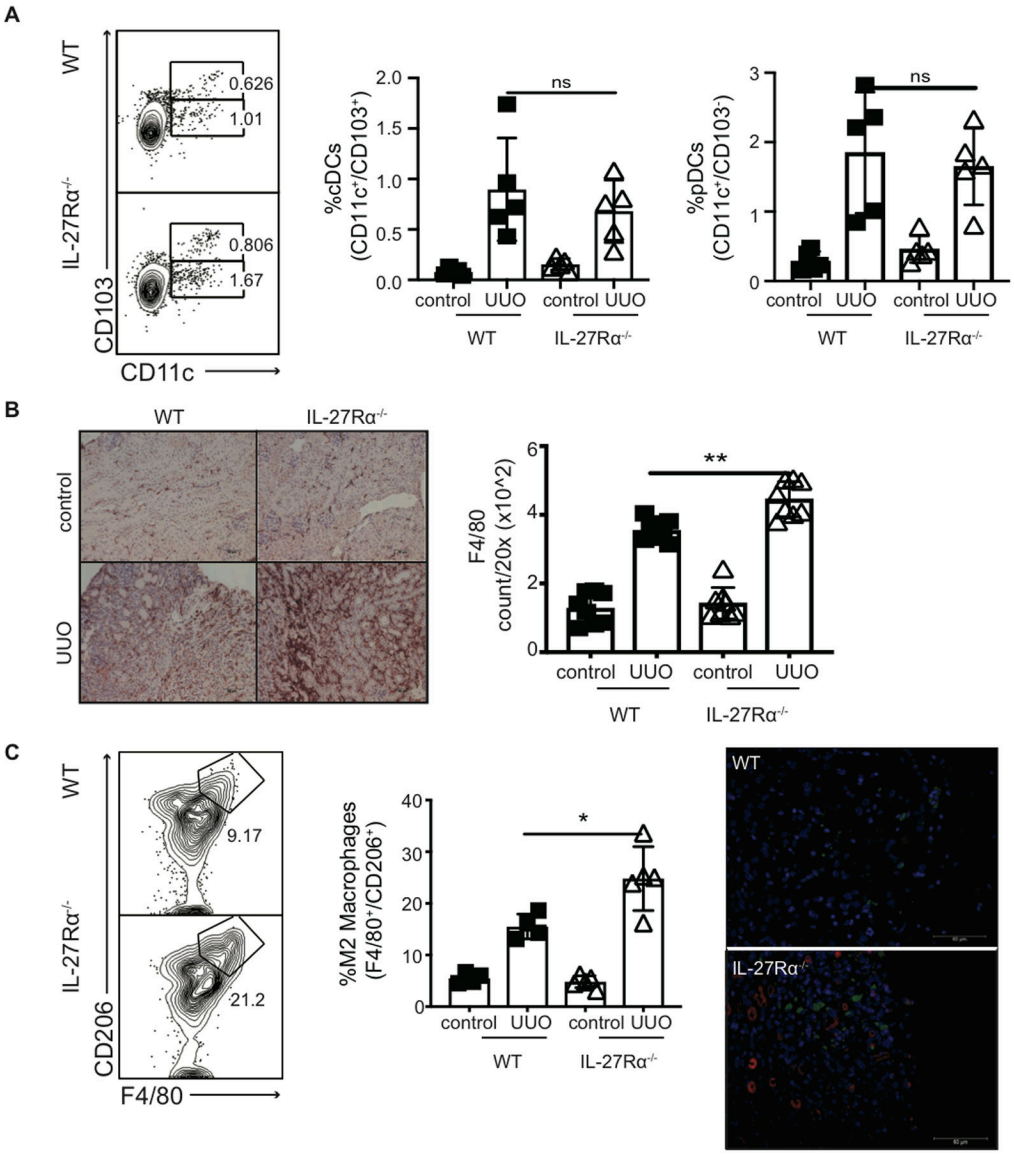

Figure 2:

WT and IL27Rα$^{-/-}$ mice underwent UUO injury. At 14 dpo kidneys were digested and cells were identified as DCs using the following gating strategy: CD3^{-}/CD19^{-}/B220^{-}/NK1.1^{-}, Ly6G^{-}/Ly6c^{-}, CD11b^{+}/MHC class 2^{+}. cDCs were identified as CD103^{+}/CX3CR1^{+} and pDCs were identified as CD103^{-}/CX3CR1^{-}. (B) Control and fibrotic kidneys were preserved in formalin 14 dpo and stained with anti-F4/80. (C) Kidneys were evaluated at 14 dpo for M2 macrophage infiltration by flow cytometry using the following gating strategy: CD3^{-}/CD19^{-}/B220^{-}/NK1.1^{-}, Ly6G^{-}/Ly6c^{-}, CD64^{+}/CD11b^{+}, CD206^{+}/F4/80^{+} and by immunofluorescence using the markers CD68 and Ym1. Groups consisted of at least four mice per group. * $p<0.05$, ** $p<0.005$, **** $p<0.0005$

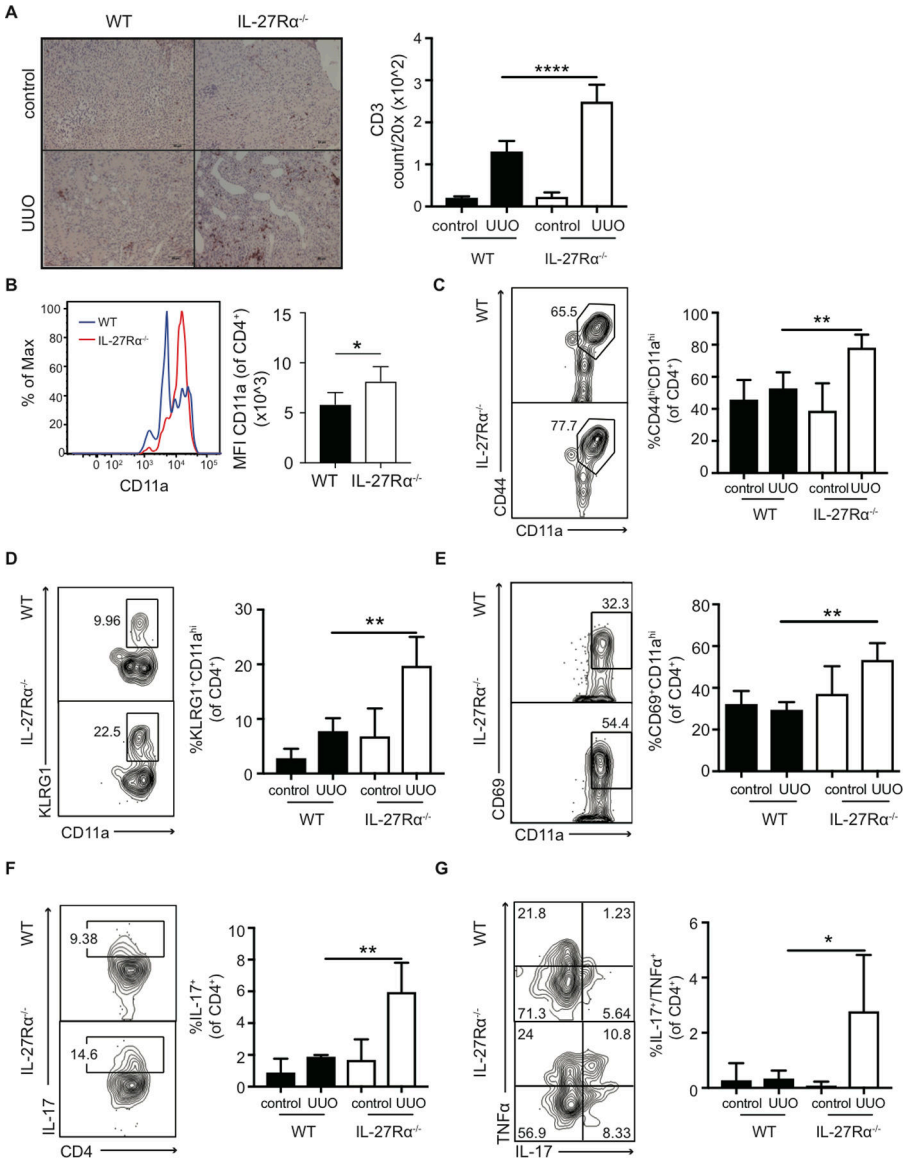

Figure 3:

WT and IL27Rα$^{-/-}$ mice underwent UUO injury. At 14 dpo (A) control and fibrotic kidneys were preserved in formalin and stained with anti-CD3. Kidneys were also digested and lymphocytes were stained with anti-CD4 and the activation markers (B) CD11a (WT versus IL-27Rα$^{-/-}$ UUO), (C) CD44, (D) KLRG1, and (E) CD69. Kidneys were evaluated for (F) IL-17 production by CD4^{+} T cells after PMA/ionomycin stimulation x4 hours. (G) Th17 cells were evaluated for production of TNFα. * $p<0.05$, ** $p<0.005$, **** $p<0.0005$

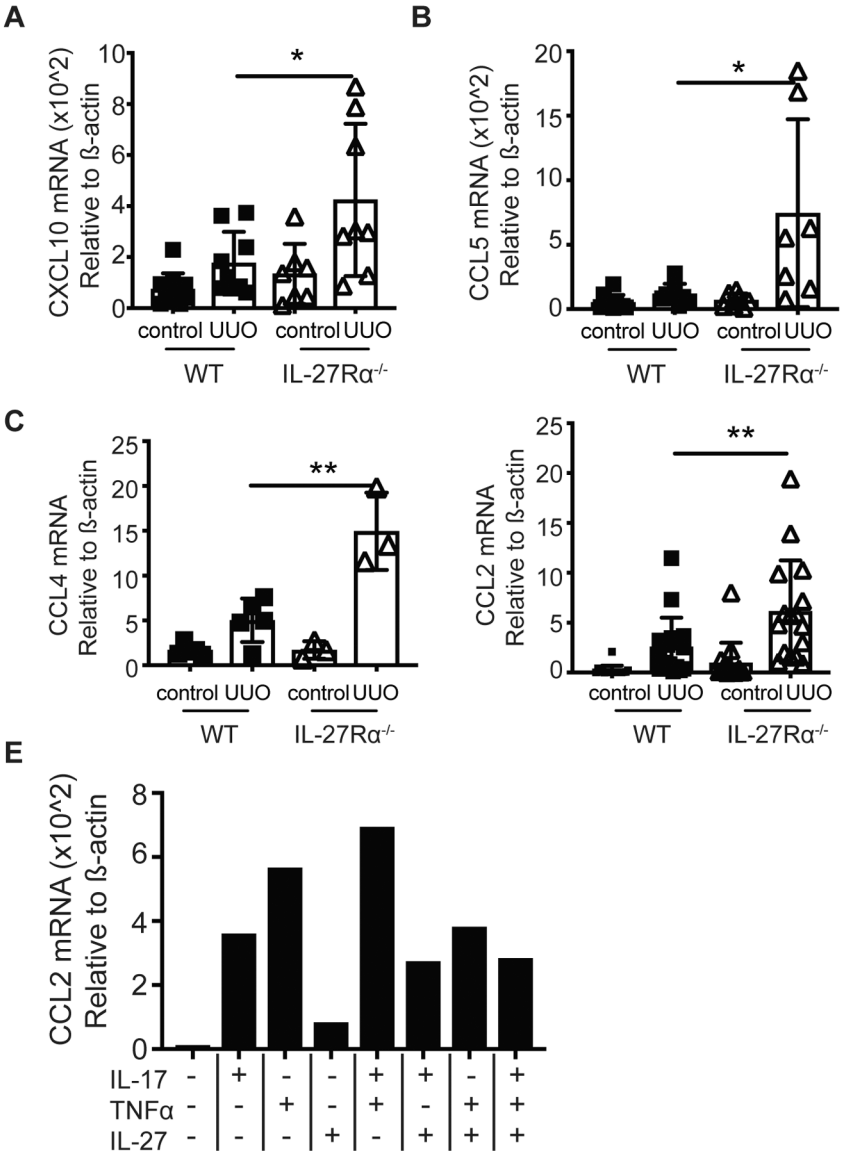

Figure 4:

WT and IL27Rα$^{-/-}$ mice underwent UUO injury. Whole kidney tissue was evaluated for (A-D) CXCL10, CCL5, CCL4, and CCL2 mRNA by RT-PCR.* $p<0.05$, ** $p<0.005$ (E) Primary renal epithelial cells were grown from WT kidneys, and IL-17 (50ng/mL), TNFα (50ng/mL), and IL-27 (50ng/nL) were added separately and in combination for 24 hours after which CCL2 mRNA was measured by RT-PCR. Similar results were observed in three experiments ($p = 0.05$).

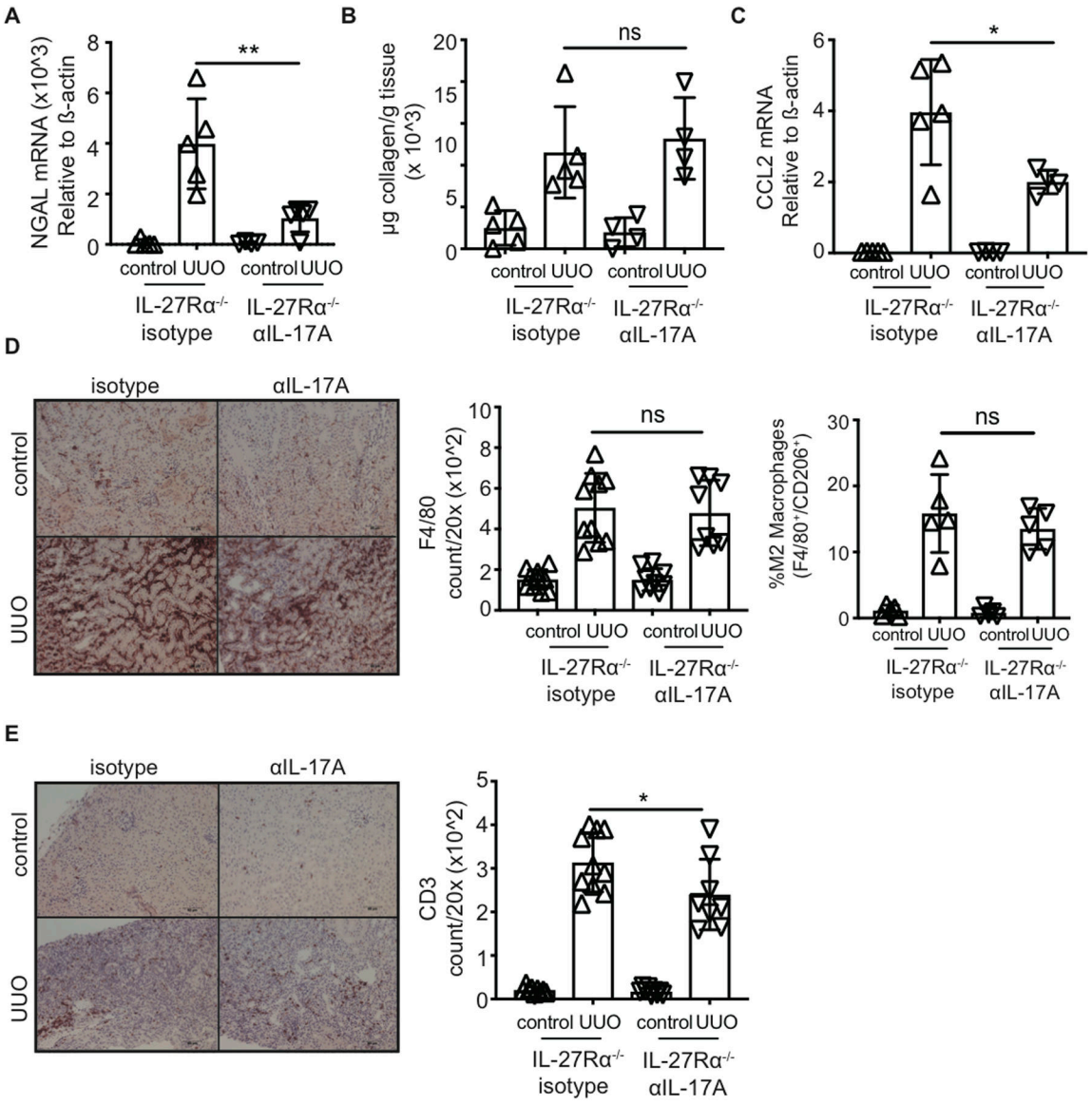

Figure 5:

IL27Rα$^{-/-}$ mice underwent UUO injury. 500µg anti-IL-17a versus IgG control were administered at 2, 4, 6, 8, 10, and 12 dpo. Kidneys were evaluated at 14 dpo for (A) injury by RT-PCR for NGAL mRNA, (B) collagen content by hydroxyproline assay, and (C) CCL2 mRNA. Control and fibrotic kidneys were preserved in formalin 14 dpo and stained with (D) anti-CD3 and (E) anti-F4/80. Kidneys were evaluated at 13 dpo for M2 macrophage infiltration by flow cytometry. * $p<0.05$

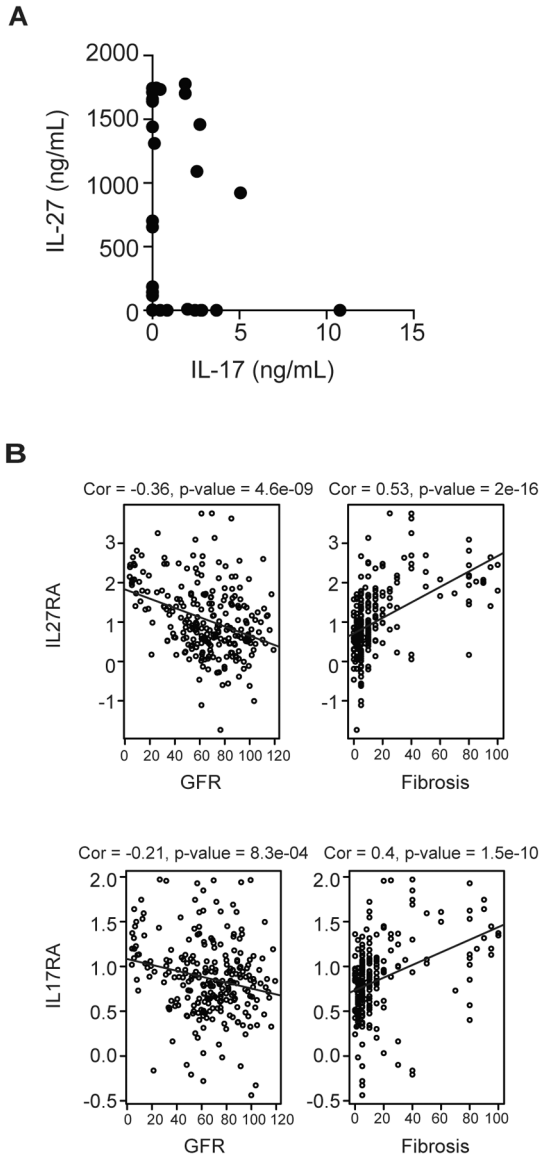

Figure 6:

(A) Serum levels of IL-27 and IL-17 in patients with CKD stage 3 or greater (CKD) plotted against each other. (B) Tubules from patients CKD were microdissected and evaluated for levels of IL-27RA and IL-17RA mRNA by disease score, glomerular filtration rate (GFR), and fibrosis as scored by a pathologist.